Mathematical Modelling and Numerical Simulation with Applications, 2022, 2(2), 88–107

https://www.mmnsa.org
ISSN Online: 2791-8564 / Open Access
https://doi.org/10.53391/mmnsa.2022.008

RESEARCH PAPER

Asymptotic behavior and semi-analytic solution of a novel compartmental biological model

Muhammad Sinan[1,*,‡], Jinsong Leng[1,‡], Misbah Anjum[2,‡] and Mudassar Fiaz[3,‡]

[1]School of Mathematical Sciences, University of Electronic Science and Technology of China, Chengdu, 611731, People's Republic of China, [2]International School of Fundamental and Frontier Sciences, University of Electronic Science and Technology of China, Chengdu, 611731, People's Republic of China, [3]Department of Mathematics, COMSATS University Islamabad, Lahore Campus, Pakistan

*Corresponding Author
‡ 202124110102@std.uestc.edu.cn, sinanmathematics@gmail.com (Muhammad Sinan); lengjs@uestc.edu.cn (Jinsong Leng); anjummisbah33@gmail.com, 202124210103@std.uestc.edu.cn (Misbah Anjum); mudassarfiaz789@gmail.com (Mudassar Fiaz)

Abstract

This study proposes a novel mathematical model of COVID-19 and its qualitative properties. Asymptotic behavior of the proposed model with local and global stability analysis is investigated by considering the Lyapunov function. The mentioned model is globally stable around the disease-endemic equilibrium point conditionally. For a better understanding of the disease propagation with vaccination in the population, we split the population into five compartments: susceptible, exposed, infected, vaccinated, and recovered based on the fundamental Kermack-McKendrick model. He's homotopy perturbation technique is used for the semi-analytical solution of the suggested model. For the sake of justification, we present the numerical simulation with graphical results.

Key words: Local asymptotic stability; global asymptotic stability; Routh-Hurwitz criterion; COVID-19; infectious disease modeling
AMS 2020 Classification: 34L30; 92D30; 37N30; 37N25

1 Introduction

Most nations throughout the world have been afflicted by the COVID-19 outbreak, and their economy has suffered as a result. There have been several cases of infection, as well as the occurrence of subsequent infection waves that have resulted in a greater number of cases than the prior wave. Although various preventative techniques and other control measures have been used to restrict the disease's spread, it is still unknown when this lethal sickness will be eradicated from the community. COVID-19 is currently infecting and killing people in the majority of the world's countries. The total number of infected cases recorded till September 4, 2021, was 220917130, including 4571624 deaths, and 197441726 [1] people recovered from COVID-19 infection. Researchers, biologists, and medical professionals are constantly attempting to develop efficient vaccines, preventions, and treatment measures for coronavirus infection management. Because there are so many different strains of this sickness, researchers are working to develop a more effective vaccine for infection prevention. According to the literature, several study publications on the virus's infection reduction have been written and published from various perspectives. We have a lot of models if we speak out that connected study on coronavirus using mathematical models. Mathematical models are the only means to determine the infection's peak and the best strategy to manage it.

In [2], researchers studied COVID-19 using a mathematical model that included Susceptible S(t), Exposed E(t), Infected I(t), Quarantine Q(t), and Recovered R(t). The goals were to examine the stability and optimal management of the concerned mathematical model for both

➤ **Received:** 24.03.2022 ➤ **Revised:** 20.06.2022 ➤ **Accepted:** 21.06.2022 ➤ **Published:** 24.06.2022

local and global stability using a third additive compound matrix technique, as well as to produce threshold values using a next-generation approach. The author created a graphic representation of the anticipated outcomes which also used the homotopy perturbation approach for the solution and for each population of the underlying model with control variables utilizing optimal control methods based on Pontryagin's maximal Principle to control the spread of COVID-19 infection in a population. In [3], researchers implemented fractional calculus on a COVID-19 mathematical model and investigated local and global stability for the stabilization of the disease in a population with an approximate solution using the Laplace-Adomian decomposition method. In [4], the authors examined the global view of the coronavirus model to real data from Ghana, as well as its cost-effective analysis with environmental changes. In [5], the authors proposed a nonlinear predictive control model and its management for coronavirus infection. In [6], the authors modeled and explored the use of medication resistance in coronavirus infection. In [7], the authors investigated the spread of coronavirus infection in China, as well as its modeling and prediction. In order to investigate the impact of lockdown in reducing coronavirus spread [8], the author examined a system of five nonlinear fractional-order equations in the Caputo sense. The hypothesised coronavirus model under lockdown's solutions were shown to exist and to be distinct using the fixed-point theorems of Schauder and Banach, respectively. Ulam-Hyers and generalised Ulam-Hyers frames for stability analysis were established.

To simulate the transmission of disease, the authors [9] looked at the SIR model with a generic incidence rate function and a nonlinear recovery rate. The influence of the health system affects the nonlinear recovery rate. The authors also established the model solution's existence, uniqueness and boundedness. They looked into the model's many steady-state solutions, stability details, and reproductive number. The research demonstrates that the free steady state is unstable otherwise and locally stable when the reproduction number is smaller than unity. The backward bifurcation phenomenon is illustrated by the model. For the transmission dynamics of HIV epidemics, the authors [10] have developed a nonlinear SEI1I2R fractional order epidemic model. The generalised mean value theorem is used to determine the model's non-negative solution. In order to determine the disease status, we obtained the fundamental reproductive number R_0, which serves as a threshold parameter. Using the fractional Routh-Hurwitz stability criterion, the asymptotically stable outcomes of equilibria are explored. While this is going on, a suitable Lyapunov function is built to evaluate the global asymptotic stability of the disease-free and endemic equilibrium point. In order to increase the concept of propagation delay, this research [11, 12] focuses on a delayed epidemic model with information-dependent vaccination.

Researchers have delved deeply into the transmission of infectious diseases or concentrated on the differential model, which solely takes into account the traits of infectious diseases themselves. The dynamic study of infectious illnesses based on vaccination rates has not received much attention. The authors [13] looked at a population model of the novel COVID-19 under ABC fractional order derivatives, and they also demonstrated enough evidence for the solution's existence and uniqueness for the model under consideration. They also demonstrated that the model has at least one solution with a stable result. The author [14] showed in this work the potential of modelling the dynamics of SARS-CoV-2 infection as a helpful support tool for measuring the population's level of compliance with the GIM and projecting the impact of corrective measures. This book [15] helps with the preliminary results and is valuable to study in the field of mathematical modelling in public health biology or public health epidemiology. In [16], the author investigated COVID-19 epidemic has had a substantial influence on children and adolescents' mental health, which should be of great concern to policymakers and practitioners around the world. This [17, 18, 19, 20, 21, 22] work examines a new mathematical model for the dynamics of Hepatitis-B virus transmission in a fractional environment in light of asymptomatic carriers and vaccination classes. Because the authors took into account both the vaccination and asymptomatic caries, this new model is more advanced than the previous models proposed for the dynamics of the Hepatitis-B virus. In this study [23, 24], the dynamics of the COVID-19 epidemic in Pakistan were examined, and a mathematical model was developed. Its fundamental and essential mathematical aspects, such as the existence and positivity of the system and its solution, were then supplied. Using fractional stability techniques, the detailed stability results for disease-free and disease-endemic equilibrium points are examined on a local and global scale.

For the dynamics of the Zika virus [25, 26] with a mutation that results in defects in newborns, a mathematical model has been devised. The threshold quantity at risk-free equilibrium and the equilibrium for Zika infection were also computed by the authors. Both locally and internationally, the stability analysis at disease-free and disease-endemic equilibrium are computed. The authors [27, 28] examined a mathematical model with slow and quick exposed cases and its impact on the model dynamics to comprehend the TB infections in the KP area of Pakistan. They also researched the fundamental math needed to model the fractional-order model. The model's stability was then examined, and it was demonstrated that the TB model is both locally and globally asymptotically stable. The examination and analysis of the suggested drinking model must also be included by the authors, who also used stochastic system perturbation to determine the solution's existence and uniqueness as well as some drinking dynamics [29]. The authors have also come to some important conclusions on how to control drinking habits at all stages, from risky to moderate and moderate to non-consumer. A discrete-time Bazykin-Berezovskaya prey-predator model's complex dynamics were described in detail by the authors [30]. Additionally, they showed that the model has a single positive interior fixed point (FPP). They also concentrated on the analytical and numerical bifurcation analysis of the interior fixed point FPP due to its biological significance.

The scientists [31] looked at an SIR model for COVID-19 in Indonesia, taking into account parameters like immunisation, treatment, application of health protocols, and coronavirus burden. Additionally, they discovered that immunisation and the application of health practices significantly limit or stop the spread of COVID-19 in Indonesia. Similar to vaccination [32] and the application of health protocols, treatment can decrease or stop the pace of COVID-19 infection. However, its impact is not as great. This study [33] presents a novel strategy for combating the COVID-19 epidemic. Using actual data from the United Kingdom, a fractional order pandemic model is created to investigate the spread of COVID-19 with and without the Omicron form and its connection to heart attacks. In [34], an optimal control model has been developed in light of the potential controls that are thought to be successful. The World Health Organization's (WHO) basic principles, such as immunisation of people, rapid testing, and early treatment of infected individuals by COVID-19, have been used to consider the four control variables in the form of preventions. In [35], this study examines the mathematical modelling of COVID-19 transmission at the fractional-order level. Using nonlinear analysis, they demonstrate the model's existence and originality. The goal of this work [36] is to thoroughly study a mathematical model for computing the nonsingular fractional order derivative-based transmissibility of a novel coronavirus (COVID-19) disease. By using the Krasnoselskii and Banach fixed point theorems, the existence and uniqueness of the proposed model have been ensured. Additionally, some stability outcomes of the Ulam-type have been developed.

In [37], the researchers studied that there was a substantial but statistically minor rise in mental health symptoms before to and during the COVID-19 pandemic in 2020, according to a study that sampled mostly European and North American people. Depressive symptoms showed bigger and longer-lasting increases, compared to anxiety disorder symptoms and measures of general mental health

functioning, which showed lower changes. It will be critical to keep track of changes in mental health (especially depression) and ensure that proper therapeutic therapy is accessible. The total rise in mental health symptoms was most evident in the first two months after the WHO proclaimed a pandemic (March 2020), before declining and returning to pre-pandemic levels by mid-2020 for most symptom kinds. In [38], the authors study COVID–19 with quarantine, isolation, and environmental viral load. They fitted the COVID–19 model to real data and calculated the parameters.

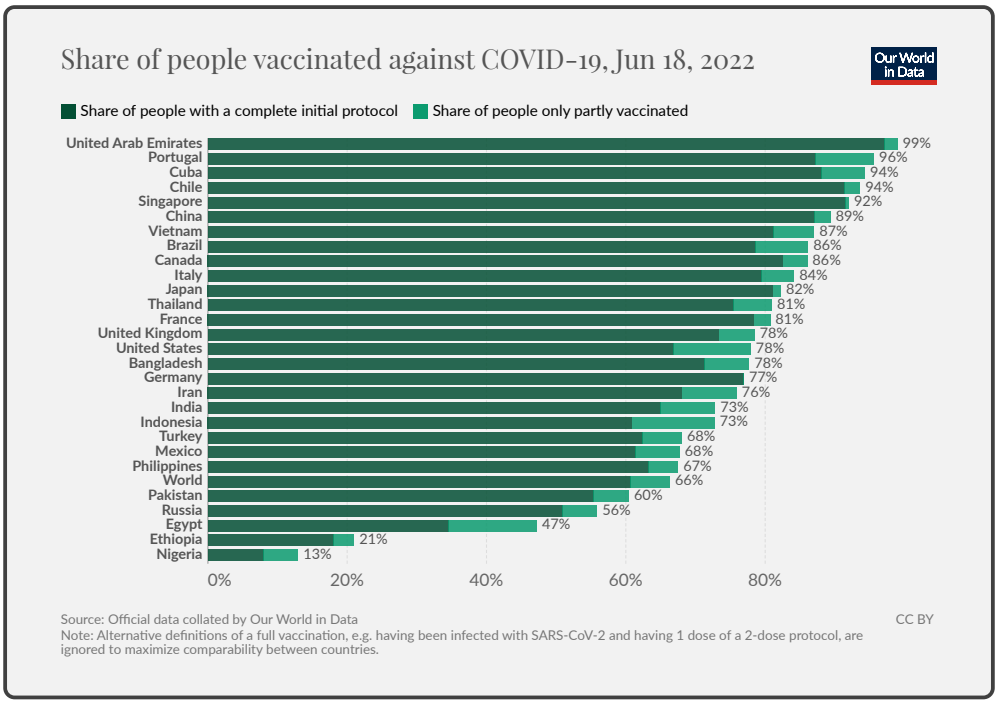

Figure 1. [39], The bar chart represents the vaccinated population with complete initial protocol and partly vaccinated for different countries

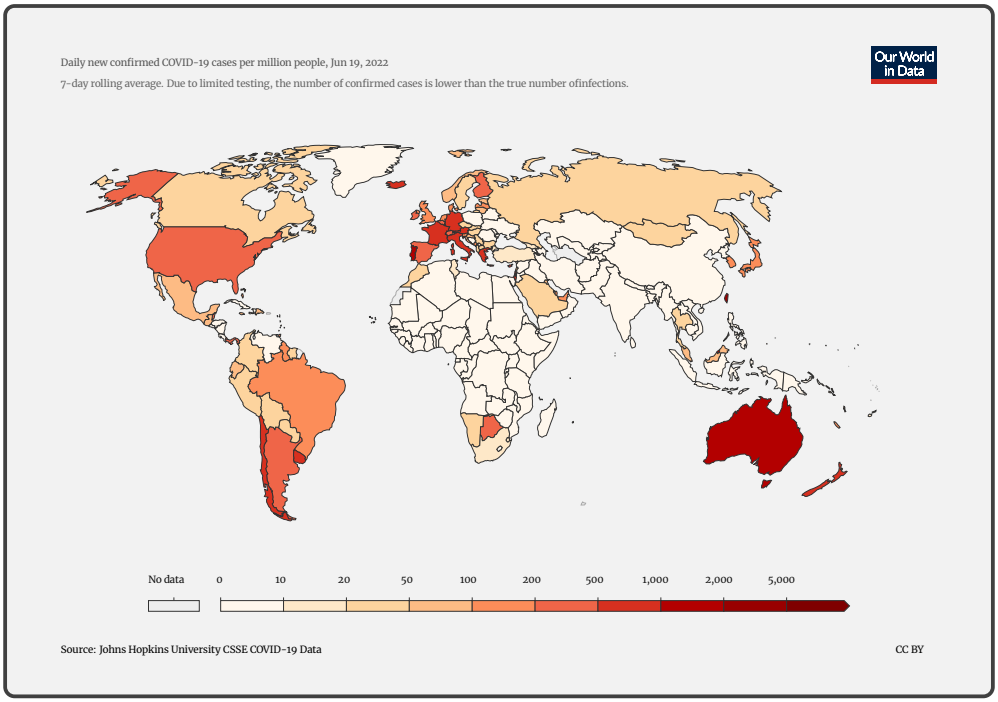

Figure 2. [39], The map of the world represents the confirmed cases of COVID–19

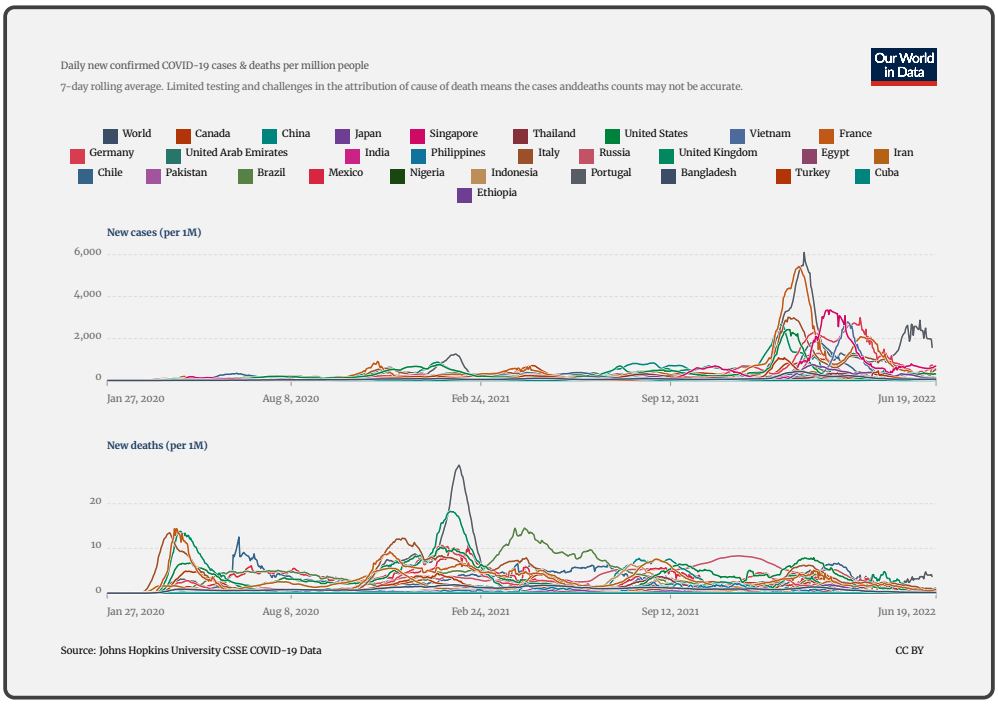

Figure 3. [39], The plots of confirmed and death cases per million people

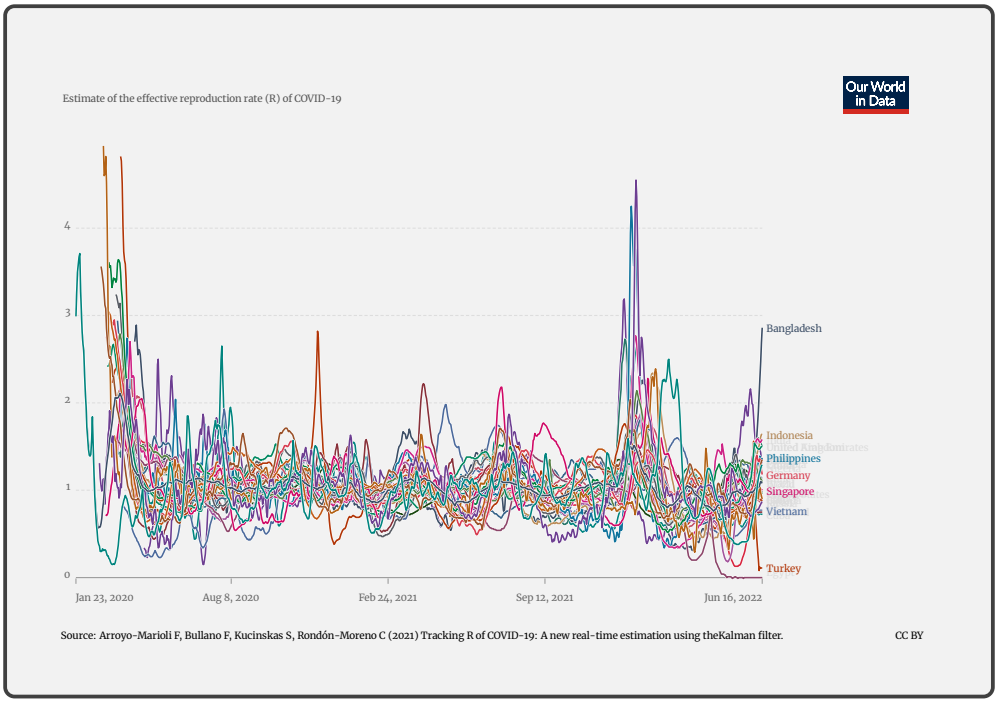

Figure 4. [39], The behaviour of basic reproduction number or reproductive rate R_0 of COVID−19 for different countries. The reproduction rate represents the average number of new infections caused by a single infected individual. If the rate is greater than 1, the infection is able to spread in the population. If it is below 1, the number of cases occurring in the population will gradually decrease to zero

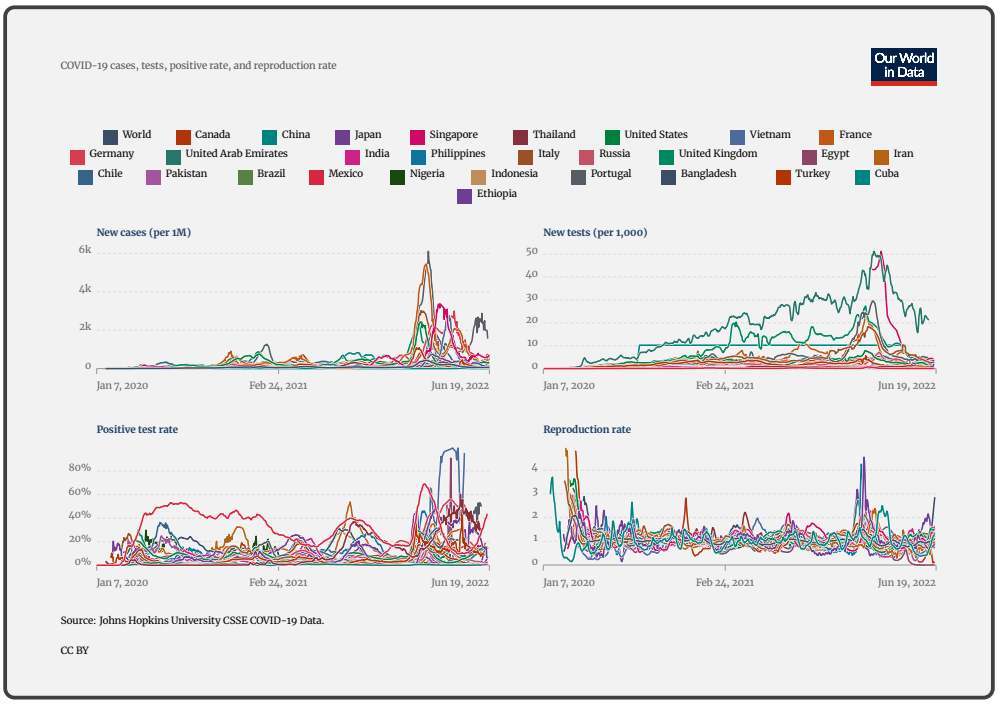

Figure 5. [39], Gallery of charts for new cases, new tests, positive test rate, and reproductive rate. 7-day rolling average. Due to limited testing, the number of confirmed cases is lower than the true number of infections. Comparisons across countries are affected by differences in testing policies and reporting methods

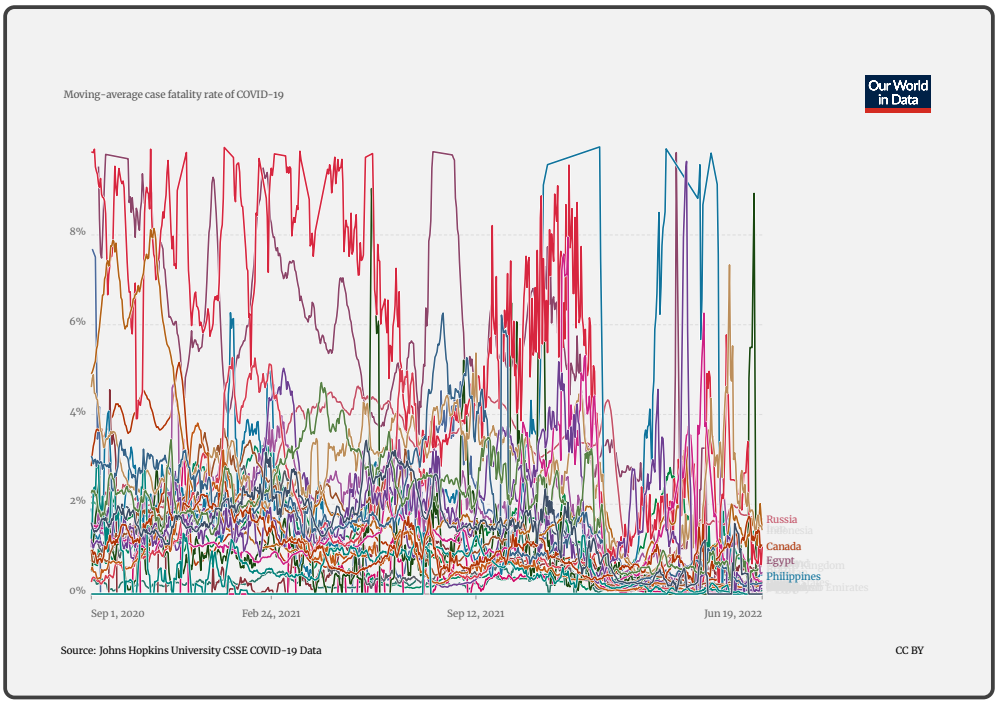

Figure 6. [39], The case fatality rate (CFR) is the ratio between confirmed deaths and confirmed cases. Our rolling-average CFR is calculated as the ratio between the 7-day average number of deaths and the 7-day average number of cases 10 days earlier.

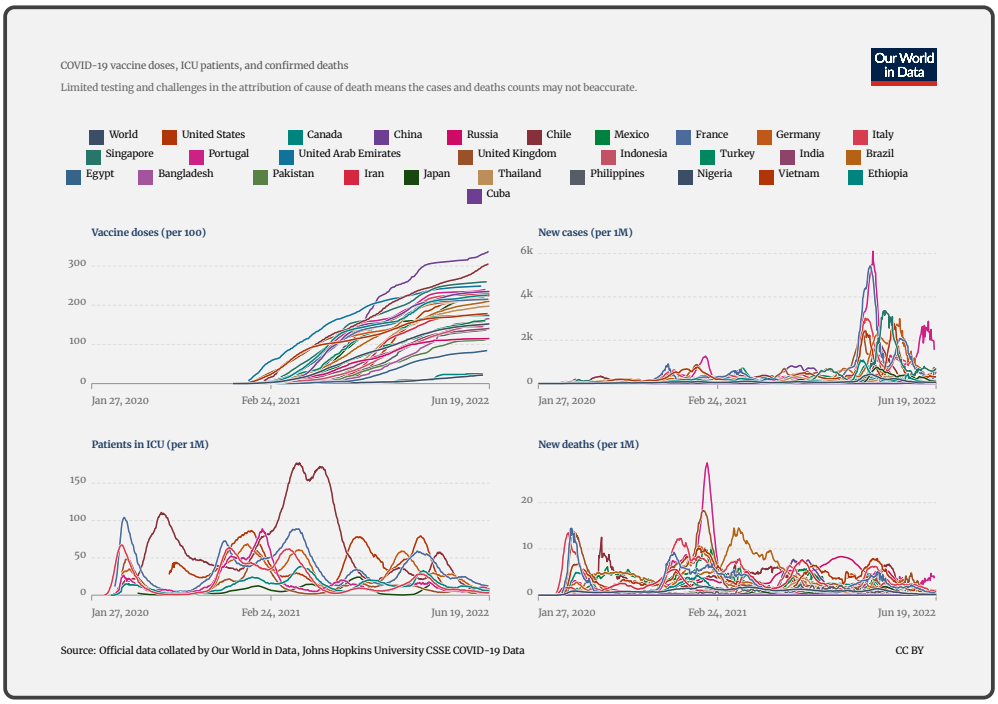

Figure 7. [39], Gallery of charts for vaccine doses, new cases, patients in ICU and New deaths

According to [40], immunization is a global success story in terms of health and development, saving millions of lives each year. Vaccines interact with your body's natural defenses to build protection, lowering your risk of contracting a disease. Your immune system reacts when you receive a vaccine. Vaccines for more than 20 life-threatening diseases are now available, allowing individuals of all ages to enjoy longer, healthier lives. Every year, vaccinations prevent 3.5-5 million fatalities from diseases such as diphtheria, tetanus, pertussis, influenza, and measles. Immunization is an indisputable human right and an important component of primary health care. It's also one of the most cost-effective health investments available. Vaccines are also essential for preventing and controlling outbreaks of infectious diseases. They are essential in the fight against antimicrobial resistance and support global health security. Despite significant advances, vaccine coverage has plateaued in recent years, and in 2020, it may potentially decline for the first time in a decade. Over the last two years, the COVID-19 pandemic and its aftermath have put pressure on health services, with 23 million children skipping vaccinations in 2020, 3.7 million more than in 2019, and the largest amount since 2009. Preliminary data from 2021 reveal continuous disruption, but on the plus side, nearly all nations had implemented COVID-19 immunization by the end of 2021, and one billion doses of COVID-19 vaccine had been supplied via COVAX by early 2022. In this paper, we investigate the asymptotic behaviour of the model locally and globally at disease–free and endemic equilibrium points. For the global stability, Lyapunov function is considered. We also use the homotopy perturbation method (HPM) to solve the non-linear dynamical system of COVID-19 semi-analytically. HPM approach was initially suggested by [41] and has since been used to solve differential and integral equations in both linear and nonlinear scenarios by [42]. In [43], the authors used the HPM to solve the nonlinear Kawahara partial differential equation semi–analytically. The HPM was used by the authors [44] to solve a set of partial differential equations. Without the use of linearization, transformation, discretization, or constrictive assumptions, the approach is used directly. We can get the conclusion that the HPM is very effective and powerful in locating analytical solutions for a variety of boundary value problems. In [45] to solve the system of rabies transmission dynamics, for resolving the generalised Zakharov equations, the HPM is suggested by the authors [46]. With potential unknown constants that can be found by imposing the boundary and initial conditions, the initial approximations can be freely chosen. For the mathematical study of obtaining the solution of a first-order in-homogeneous partial differential equation $u_x(x,y) + a(x,y)u_y(x,y) + b(x,y)g(u) = f(x,y)$, a new homotopy technique is proposed [47]. This new method is developed by combining the decomposition of a source function and the HPM.

COVID-19 mathematical model formulation

In this section, we modifying Susceptible, Infected, and Recovered (SIR) model [9, 31] for COVID-19 infection with the implementation of the vaccination class/compartment such that:

$$\begin{aligned} \frac{dS(t)}{dt} &= -\beta S(t)I(t), \\ \frac{dI(t)}{dt} &= \beta S(t)I(t) - \gamma I(t), \\ \frac{dI(t)}{dt} &= \gamma I(t). \end{aligned} \tag{1}$$

For mathematical modelling of the model, we provide the compartmental diagram below:

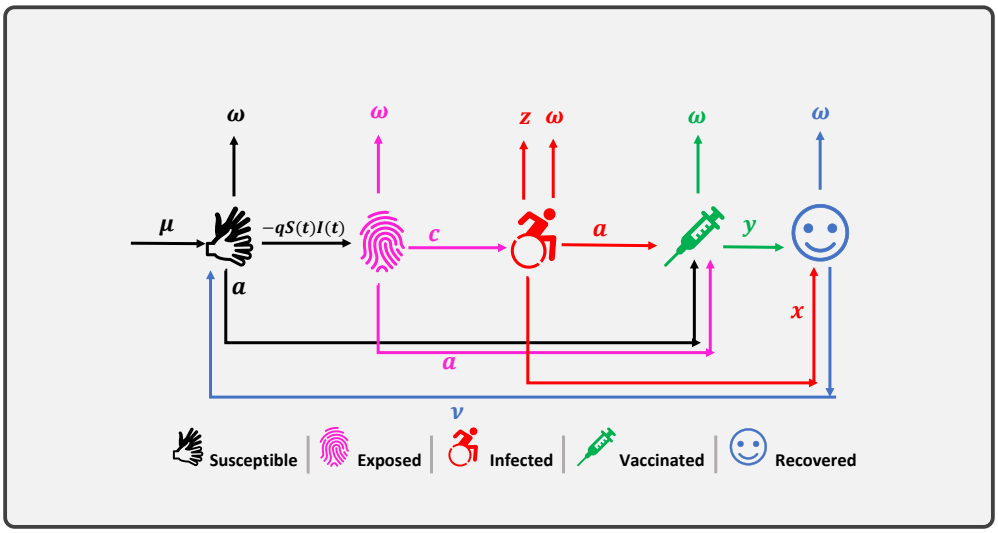

Figure 8. Compartmental diagram of COVID–19 model

Based on the compartmental diagram (8), the following model is proposed:

$$\left.\begin{aligned}
\frac{dS(t)}{dt} &= \mu - qS(t)I(t) - (\omega + a)S(t) + \nu R(t),\\
\frac{dE(t)}{dt} &= qS(t)I(t) - (c + \omega + a)E(t),\\
\frac{dI(t)}{dt} &= cE(t) - (a + \omega + x + z)I(t),\\
\frac{dV(t)}{dt} &= aI(t) - (\omega + y)V(t) + aE(t) + aS(t),\\
\frac{dR(t)}{dt} &= xI(t) + yV(t) - (\omega + \nu)R(t),
\end{aligned}\right\} \tag{2}$$

with $S(0) \geq 0$, $E(0) \geq 0$, $I(0) \geq 0$, $V(0) \geq 0$, and $R(0) \geq 0$. Also, here SEIVR represents Susceptible, Exposed, Infected, Vaccinated and Recovered compartments, respectively. Also, μ is the rate of recruitment, q is the rate of transmission, ω is the rate of natural death, a is the rate of vaccination, ν is the rate of loss of immunity, c is the rate of infection of Exposed population, x is the recovery rate of Infected population, z is the death rate of Infected population due to the disease, y is the immunity of vaccinated population.

More assumptions

In order to build a new model, we must make assumptions in order to simplify reality. The Kermack–McKendrick model's primary premise is that diseased people are likewise contagious. The overall population size remains constant. There are only two types of death in the population: natural death and death due to the disease. The population is open to accept new individuals from outside the existing population. The infected individuals can be recovered with hospitalization. The parameters of are non-negative and $N(t) = S(t) + E(t) + I(t) + V(t) + R(t)$ where $N(t)$ stands for the total population at the time t such that $t \in \Omega := [0, T]$ for $T > 0$.

2 Equilibrium points and their stability analysis

The disease–free equilibrium point is computed as:

$$E^0 = \left(S^0, 0, 0, V^0, R^0\right), \tag{3}$$

where,

$$\left.\begin{aligned}
S^0 &= \frac{\mu\left(\nu\omega + \nu y + \omega y + \omega^2\right)}{\nu\omega^2 + \omega^2 q + \omega^2 y + \omega^3 - a\nu y + \nu\omega q + \nu\omega y + \nu q y + \omega q y},\\
V^0 &= \frac{a\mu(\nu + \omega)}{\nu\omega^2 + \omega^2 q + \omega^2 y + \omega^3 - a\nu y + \nu\omega q + \nu\omega y + \nu q y + \omega q y},\\
R^0 &= \frac{a\mu y}{\nu\omega^2 + \omega^2 q + \omega^2 y + \omega^3 - a\nu y + \nu\omega q + \nu\omega y + \nu q y + \omega q y}.
\end{aligned}\right\} \tag{4}$$

The basic reproduction number at the disease-free equilibrium point for the model (2) is computed below:

$$R_0 = \frac{cqS^0}{(a+c+\omega)(a+\omega+x+z)}, \tag{5}$$

where,

$$S^0 = \frac{\mu\left(\nu\omega+\nu y+\omega y+\omega^2\right)}{\nu\omega^2+\omega^2 q+\omega^2 y+\omega^3-a\nu y+\nu\omega q+\nu\omega y+\nu q y+\omega q y}. \tag{6}$$

Theorem 1 *The COVID-19 model at the disease-free equilibrium point E^0 is locally asymptotically stable if $R_0 < 1$, otherwise unstable.*

Proof 1 *The Jacobian matrix of the model (2) is computed as:*

$$J(E^0) = \begin{bmatrix} -a-\omega & 0 & -qS^0 & 0 & \nu \\ 0 & -a-c-\omega & qS^0 & 0 & 0 \\ 0 & c & -a-\omega-x-z & 0 & 0 \\ a & a & a & -\omega-y & 0 \\ 0 & 0 & x & y & -\nu-\omega \end{bmatrix}. \tag{7}$$

After a little simplification using the row reduction process, then the matrix (7) takes the form:

$$J(E^0) = \begin{bmatrix} -a-\omega & 0 & -qS^0 & 0 & \nu \\ 0 & -a-c-\omega & qS^0 & 0 & 0 \\ 0 & 0 & cqS^0-(a+\omega+x+z)(a+c+\omega) & 0 & 0 \\ 0 & 0 & [a(a+\omega)-aqS^0](a+c+\omega)+qS^0a(a+\omega) & -(\omega+y)(a+\omega)(a+c+\omega) & 0 \\ 0 & 0 & x & y & -\nu-\omega \end{bmatrix}. \tag{8}$$

Clearly, we get all the eigenvalues such that $\lambda_1 = -a-\omega$, $\lambda_2 = -a-c-\omega$, $\lambda_3 = -\nu-\omega$, $\lambda_4 = -(\omega+y)(a+\omega)(a+c+\omega)$, and $\lambda_5 = cqS^0-(a+\omega+x+z)(a+c+\omega)$. As we see that the eigenvalues other than λ_5 are negative while $\lambda_5 < 0$ if $cqS^0-(a+\omega+x+z)(a+c+\omega) < 0$ implies that $cqS^0 < (a+\omega+x+z)(a+c+\omega)$ furthermore $cqS^0/(a+\omega+x+z)(a+c+\omega) < 1 \Rightarrow R_0 < 1$. Hence the model (2) is locally asymptotically stable around disease−free equilibrium point E_0 if $R_0 < 1$. This completes the proof.

Theorem 2 *The COVID-19 model at the disease-endemic equilibrium point E^* is locally asymptotically stable if $R_0 > 1$, otherwise unstable.*

Proof 2 *The Jacobian matrix of the model (2) is computed as:*

$$J(E^*) = \begin{bmatrix} -a-\omega-qI^* & 0 & -qS^* & 0 & \nu \\ qI^* & -a-c-\omega & qS^* & 0 & 0 \\ 0 & c & -a-\omega-x-z & 0 & 0 \\ a & a & a & -\omega-y & 0 \\ 0 & 0 & x & y & -\nu-\omega \end{bmatrix}. \tag{9}$$

Computing the characteristic equation of Jacobian matrix (9), such that:

$$\lambda^5 + a_1\lambda^4 + a_2\lambda^3 + a_3\lambda^2 + a_4\lambda + a_5, \tag{10}$$

where, the coefficients are the following:

$$
\begin{aligned}
a_1 &= (3a + c + \nu + 5\omega + x + y + z + I^*q)\,,\\
a_2 &= (2ac + 3a\nu + 12a\omega + c\nu + 4c\omega + 2ax + 3ay + 2az + cx + cy + cz + 4\nu\omega + \nu x + 4\omega x + \nu y + 4\omega y\\
&\quad + \nu z + 4\omega z + xy + yz + 3a^2 + 10\omega^2 + 2I^*aq + I^*cq - Scq + I^*\nu q + 4I^*\omega q + Iqx + Iqy + Iqz),\\
a_3 &= (a^2c + 3a^2\nu + 18a\omega^2 + 9a^2\omega + 6c\omega^2 + a^2x + 3a^2y + a^2z + 6\nu\omega^2 + 6\omega^2x\\
&\quad + 6\omega^2y + 6\omega^2z + a^3 + 10\omega^3 + 2ac\nu + 6ac\omega + acx + 2acy + acz + 9a\nu\omega + 3c\nu\omega + 2a\nu x\\
&\quad + 6a\omega x + 2a\nu y + 9a\omega y + 2a\nu z + c\nu x + 6a\omega z + 3c\omega x + c\nu y + 3c\omega y + c\nu z + 3c\omega z\\
&\quad + 2axy + 2ayz + cxy + 3\nu\omega x + cyz + 3\nu\omega y + 3\nu\omega z + \nu xy + 3\omega xy + \nu yz + 3\omega yz + I^*a^2q\\
&\quad + 6I^*\omega^2q + I^*\nu qx + 3I^*\omega qx + I^*\nu qy + 3I^*\omega qy + I^*\nu qz\\
&\quad + 3I^*\omega qz + I^*qxy + I^*qyz + I^*acq - Sacq + 2I^*a\nu q + 6I^*a\omega q + I^*c\nu q\\
&\quad + 3I^*c\omega q + I^*aqx + 2I^*aqy + I^*aqz + I^*cqx - Sc\nu q + I^*cqy - 3Sc\omega q + I^*cqz + 3I^*\nu\omega q - Scqy),\\
a_4 &= (a^3\nu + 12a\omega^3 + 2a^3\omega + 4c\omega^3 + a^3y + 4\nu\omega^3 + 4\omega^3x + 4\omega^3y + 4\omega^3z + 5\omega^4\\
&\quad + 9a^2\omega^2 + a^2\nu x + 6a\omega^2x + 2a^2\omega x + a^2\nu y + 9a\omega^2y + 6a^2\omega y + a^2\nu z + 6a\omega^2z + 3c\omega^2x\\
&\quad + 2a^2\omega z + 3c\omega^2y + 3c\omega^2z + a^2xy + a^2yz + 3\nu\omega^2x + 3\nu\omega^2y + 3\nu\omega^2z + 3\omega^2xy + 3\omega^2yz\\
&\quad + 4I^*\omega^3q + a^2c\nu + 6ac\omega^2 + 2a^2c\omega + a^2cy + 9a\nu\omega^2 + 6a^2\nu\omega + 3c\nu\omega^2 + 4ac\nu\omega\\
&\quad + ac\nu x + 2ac\omega x + ac\nu y + 4ac\omega y + ac\nu z + 2ac\omega z + acxy + 4a\nu\omega x + acyz + 4a\nu\omega y + 4a\nu\omega z + 2c\nu\omega x\\
&\quad + 2c\nu\omega y + 2c\nu\omega z + a\nu xy + 4a\omega xy + a\nu yz + c\nu xy + 4a\omega yz + 2c\omega xy + c\nu yz + 2c\omega yz + 2\nu\omega xy\\
&\quad + 2\nu\omega yz + I^*a^2\nu q + 6I^*a\omega^2q + 2I^*a^2\omega q + 3I^*c\omega^2q + I^*a^2qy\\
&\quad - 3Sc\omega^2q + 3I^*\nu\omega^2q + 3I^*\omega^2qx + 3I^*\omega^2qy + 3I^*\omega^2qz + I^*ac\nu q\\
&\quad + 2I^*ac\omega q - Sac\nu q + I^*acqy - 2Sac\omega q + 4I^*a\nu\omega q + 2I^*c\nu\omega q - Sacqy + I^*a\nu qx\\
&\quad + 2I^*a\omega qx + I^*a\nu qy + 4I^*a\omega qy + I^*a\nu qz + 2I^*a\omega qz + 2I^*c\omega qx + I^*c\nu qy\\
&\quad - 2Sc\nu\omega q + 2I^*c\omega qy + I^*c\nu qz + 2I^*c\omega qz + I^*aqxy + I^*aqyz + I^*cqxy - Sc\nu qy\\
&\quad - 2Sc\omega qy + 2I^*\nu\omega qx + I^*cqyz + 2I^*\nu\omega qy + 2I^*\nu\omega qz + I^*\nu qxy + 2I^*\omega qxy + I^*\nu qyz + 2I^*\omega qyz),\\
a_5 &= 3a\omega^4 + c\omega^4 + \nu\omega^4 + \omega^4x + \omega^4y + \omega^4z + \omega^5 + 3a^2\omega^3 + a^3\omega^2 + 2a\omega^3x + 3a\omega^3y\\
&\quad + a^3\omega y + 2a\omega^3z + c\omega^3x + c\omega^3y + c\omega^3z + \nu\omega^3x + \nu\omega^3y + \nu\omega^3z + \omega^3xy + \omega^3yz\\
&\quad + a^2c\omega^2 + 3a^2\nu\omega^2 + a^2\omega^2x + 3a^2\omega^2y + a^2\omega^2z + I^*\omega^4q + 2ac\omega^3 + 3a\nu\omega^3 + a^3\nu\omega + c\nu\omega^3\\
&\quad + 2I^*a\omega^3q + I^*c\omega^3q - Sc\omega^3q + I^*\nu\omega^3q + I^*\omega^3qx + 2ac\nu\omega^2 + a^2c\nu\omega + I^*\omega^3qy\\
&\quad + I^*\omega^3qz + ac\omega^2x + 2ac\omega^2y + a^2c\omega y + ac\omega^2z + 2a\nu\omega^2x + a^2\nu\omega x + 2a\nu\omega^2y + a^2\nu\omega y\\
&\quad + 2a\nu\omega^2z + c\nu\omega^2x + a^2\nu\omega z + c\nu\omega^2y + c\nu\omega^2z + 2a\omega^2xy + a^2\omega xy + 2a\omega^2yz + c\omega^2xy + a^2\omega yz\\
&\quad + c\omega^2yz + \nu\omega^2xy + \nu\omega^2yz + I^*a^2\omega^2q + ac\nu\omega x + ac\nu\omega y + ac\nu\omega z + ac\omega xy + ac\omega yz + a\nu\omega xy\\
&\quad + a\nu\omega yz + c\nu\omega xy + c\nu\omega yz + I^*ac\omega^2q - Sac\omega^2q + 2I^*a\nu\omega^2q + I^*a^2\nu\omega q\\
&\quad + I^*c\nu\omega^2q + I^*a\omega^2qx + 2I^*a\omega^2qy + I^*a^2\omega qy + I^*a\omega^2qz + I^*c\omega^2qx - Sc\nu\omega^2q\\
&\quad + I^*c\omega^2qy + I^*c\omega^2qz - Sc\omega^2qy + I^*\nu\omega^2qx + I^*\nu\omega^2qy + I^*\nu\omega^2qz\\
&\quad + I^*\omega^2qxy + I^*\omega^2qyz + I^*ac\nu\omega q - Sac\nu\omega q + I^*ac\omega qy - Sac\omega qy + I^*a\nu\omega qx\\
&\quad + I^*a\nu\omega qy + I^*a\nu\omega qz + I^*c\nu\omega qy + I^*c\nu\omega qz + I^*a\omega qxy + I^*a\omega qyz\\
&\quad + I^*c\omega qxy - Sc\nu\omega qy + I^*c\nu qyz + I^*c\omega qyz + I^*\nu\omega qxy + I^*\nu\omega qyz.
\end{aligned}
\tag{11}
$$

Apparently, for positive endemic equilibrium point E^* $(S^*, E^*, I^*, V^*, R^*)$ is locally asymptotically stable [48] if the following inequalities are satisfied

$$
det_1 = a_5 > 0,\quad det_2 = \begin{vmatrix} a_1 & 1 \\ a_3 & a_2 \end{vmatrix} > 0,\quad det_3 = \begin{vmatrix} a_1 & 1 & 0 \\ a_3 & a_2 & a_1 \\ 0 & a_4 & a_3 \end{vmatrix} > 0,\quad \text{and}\quad det_4 = \begin{vmatrix} a_1 & 1 & 0 & 0 \\ a_3 & a_2 & a_1 & 1 \\ a_5 & a_4 & a_3 & a_2 \\ 0 & 0 & a_5 & a_4 \end{vmatrix} > 0. \tag{12}
$$

Considering the coefficients (11) *of the characteristic equation* (10), *the Routh–Hurwitz criterion [49] is satisfied because all of the coefficients are positive and inequalities* (12) *are satisfied. As a result, all the eigenvalues are negative or have negative real parts and $R_0 > 1$. Hence, the model is locally asymptotically stable around the disease-endemic equilibrium point, E^*.*

3 Global stability analysis

For the endemic Lyapunov function, $\{S, E, I, V, R\}$, $\dot{L} < 0$ is the endemic equilibrium E^*.

Theorem 3 *[10, 11, 15] If $R_0 > 1$, the endemic equilibrium point E^* of the model* (2) *is globally asymptotically stable otherwise unstable.*

Proof 3 *For proof, the Lyapunov function can be written as*

$$L(S^*, E^*, I^*, V^*, R^*) = \left(S - S^* - S^* \log \frac{S^*}{S}\right) + \left(E - E^* - E^* \log \frac{E^*}{E}\right) + \left(V - V^* - V^* \log \frac{V^*}{V}\right) + \left(I - I^* - I^* \log \frac{I^*}{I}\right) + \left(R - R^* - R^* \log \frac{R^*}{R}\right). \tag{13}$$

Therefore, applying the derivative respect to t on both sides yields

$$\frac{dL}{dt} = \left(\frac{S - S^*}{S}\right)\dot{S} + \left(\frac{E - E^*}{E}\right)\dot{E} + \left(\frac{I - I^*}{I}\right)\dot{I} + \left(\frac{V - V^*}{V}\right)\dot{V} + \left(\frac{R - R^*}{R}\right)\dot{R}, \tag{14}$$

which implies that

$$\left.\begin{aligned}\frac{dL}{dt} &= \left(\frac{S - S^*}{S}\right)(\mu - qS(t)I(t) - (\omega + a)S(t) + \nu R(t)) \\ &+ \left(\frac{E - E^*}{E}\right)(qS(t)I(t) - (c + \omega + a)E(t)) \\ &+ \left(\frac{I - I^*}{I}\right)(cE(t) - (a + \omega + x + z)I(t)) \\ &+ \left(\frac{V - IV^*}{V}\right)(aI(t) - (\omega + y)V(t) + aE(t) + aS(t)) \\ &+ \left(\frac{R - R^*}{R}\right)(xI(t) + yV(t) - (\omega + \nu)R(t)).\end{aligned}\right\} \tag{15}$$

Furthermore,

$$\left.\begin{aligned}\frac{dL}{dt} &= \mu - \frac{\mu S^*}{S} - \frac{qI}{S}(S - S^*)^2 + \frac{q}{S}I^*(S - S^*)^2 - \frac{(\omega + a)}{S}(S - S^*)^2 + \nu R - \nu R^* - \frac{VS^*R}{S} + \frac{VS^*R^*}{S} \\ &- \frac{qE^*I^*}{E} + qSI - qS^*I - \frac{qE^*I^*S^*}{E} - \frac{(c + \omega + a)}{E}(E - E^*)^2 + \frac{cI^*E}{I} - \frac{cE^*I^*}{I} \\ &+ cE - cE^* - (a + \omega + x + z)\frac{(I - I^*)^2}{I} + aI - aI^* - \frac{aVI^*}{V} - \frac{aV^*I^*}{V} - (\omega + y)\frac{(V - V^*)^2}{V} \\ &+ aE - aE^* - \frac{aV^*E}{V} - \frac{aE^*V^*}{V}.\end{aligned}\right\} \tag{16}$$

Now, Eq. (16) can be written in the form of:

$$\frac{dL}{dt} = \digamma - \alpha, \tag{17}$$

where,

$$\digamma = \mu + \frac{q}{S}I^*(S - S^*)^2 + \nu R + \frac{VS^*R^*}{S} + qSI + \frac{cI^*E}{I} + cE + aI + aE, \tag{18}$$

and

$$\left.\begin{aligned}\alpha &= -\frac{\mu S^*}{S} - \frac{qI}{S}(S - S^*)^2 - \frac{(\omega + a)}{S}(S - S^*)^2 - \nu R^* - \frac{VS^*R}{S} \\ &- \frac{qE^*I^*}{E} - qS^*I - \frac{qE^*I^*S^*}{E} - \frac{(c + \omega + a)}{E}(E - E^*)^2 - \frac{cE^*I^*}{I} \\ &- cE^* - (a + \omega + x + z)\frac{(I - I^*)^2}{I} - aI^* - \frac{aVI^*}{V} - \frac{aV^*I^*}{V} \\ &- (\omega + y)\frac{(V - V^*)^2}{V} - aE^* - \frac{aV^*E}{V} - \frac{aE^*V^*}{V}.\end{aligned}\right\} \tag{19}$$

Eventually, if $\digamma < \alpha$ then $\frac{dL}{dt} < 0$ while using $S = S^*, E = E^*, I = I^*, V = V^*$, and $R = R^*$, $0 = \digamma - \alpha$ implies that $\frac{dL}{dt} = 0$. Also, for the suggested model (2) we are looking the largest compact invariant set $\left\{(S^*, E^*, I^*, V^*, R^*) \in \Omega : \frac{dL}{dt} = 0\right\}$ is the endemic equilibrium point $E^* = (S^*, E^*, I^*, V^*, R^*)$ of the considered model. Thus, the model (2) is stable in Ω if $R_0 > 1$ and $\digamma < \alpha$.

4 Homotopy perturbation method

Consider a general type problem given by

$$A(\mu) - f(r) = 0, \quad r \in \Omega, \tag{20}$$

with the boundary conditions as

$$\beta\left(\mu, \frac{\partial \mu}{\partial n}\right) = 0, r \in \Gamma, \tag{21}$$

where A is a general differential operator, β is a boundary operator, $f(r)$ is a known analytic function, and Γ is the boundary of the domain Ω. The operator A is divided into linear part L and nonlinear part N. Therefore, (20) can be written as

$$L(\mu) + N(u) - f(r) = 0. \tag{22}$$

By HPM, we can construct a homotopy as

$$v(r, \mathbf{s}) : \Omega \times [0, 1] \to R, \tag{23}$$

satisfying

$$H(v, \mathbf{s}) = (1 - \mathbf{s})[L(v) - L(\mu)] + \mathbf{s}[A(v - f(r))] = 0, \tag{24}$$

which is also equivalent to

$$H(v, \mathbf{s}) = L(v) - L(\mu_0) + \mathbf{s}L(v_0) + \mathbf{s}[N(v) - f(r)] = 0, \tag{25}$$

where $\mathbf{s} \in [0;1]$ is an embedding parameter, and μ_0 is the initial approximation of the given equation that satisfies the boundary conditions; we have

$$\begin{aligned} H(v, 0) &= L(v) - L(\mu_0) = 0, \\ H(v, 1) &= A(v) - f(r) = 0. \end{aligned} \tag{26}$$

Keeping these points, we construct the required solution to equation (22) as

$$v = v_0 + \mathbf{s}^1 v_1 + \mathbf{s}^2 v_2 + \mathbf{s}^3 v_3 + \cdots. \tag{27}$$

Furthermore, by taking the limit as $p \to 1$ in the approximation equation (27), one has

$$\lim_{\mathbf{s}\to 1} v = \lim_{\mathbf{s}\to 1} v_0 + \mathbf{s}^1 v_1 + \mathbf{s}^2 v_2 + \mathbf{s}^3 v_3 + \cdots, \tag{28}$$

which yields

$$v = v_0 + v_1 + v_2 + v_3 + \cdots. \tag{29}$$

Equation (29) represents the semianalytic solution of the problem equation (20).

5 Approximate solution of the proposed COVID-19 model

Applying homotopy on the model (2)

$$\left.\begin{aligned} \mathcal{D}S(t) - \mathcal{D}S(0) &= \mathbf{s}[\mu - qS(t)I(t) - (\omega + a)S(t) + \nu R(t)], \\ \mathcal{D}E(t) - \mathcal{D}E(0) &= \mathbf{s}[qS(t)I(t) - (c + \omega + a)E(t)], \\ \mathcal{D}I(t) - \mathcal{D}I(0) &= \mathbf{s}[cE(t) - (a + \omega + x + z)I(t)], \\ \mathcal{D}V(t) - \mathcal{D}V(0) &= \mathbf{s}[aI(t) - (\omega + y)V(t) + aE(t) + aS(t)], \\ \mathcal{D}R(t) - \mathcal{D}R(0) &= \mathbf{s}[xI(t) + yV(t) - (\omega + \nu)R(t)]. \end{aligned}\right\} \tag{30}$$

Assume series solution to the model (2), such that

$$\left.\begin{aligned} S(t) &= S(0) + \mathbf{s}S_1(t) + \mathbf{s}^2 S_2(t) + \mathbf{s}^3 S_3(t) + \cdots, \\ E(t) &= E(0) + \mathbf{s}E_1(t) + \mathbf{s}^2 E_2(t) + \mathbf{s}^3 E_3(t) + \cdots, \\ I(t) &= I(0) + \mathbf{s}I_1(t) + \mathbf{s}^2 I_2(t) + \mathbf{s}^3 I_3(t) + \cdots, \\ V(t) &= V(0) + \mathbf{s}V_1(t) + \mathbf{s}^2 V_2(t) + \mathbf{s}^3 V_3(t) + \cdots, \\ R(t) &= R(0) + \mathbf{s}R_1(t) + \mathbf{s}^2 R_2(t) + \mathbf{s}^3 R_3(t) + \cdots. \end{aligned}\right\} \tag{31}$$

Now by comparison we get $\mathbf{s}^0, \mathbf{s}^1, \mathbf{s}^2, \cdots$ by using system of equations (31) in (30), we have:

Zeroth-order problem

$$\left.\begin{aligned}
\mathbf{s}^0 &:= \mathcal{D}S(0) = \mathcal{D}S_0,\\
\mathbf{s}^0 &:= \mathcal{D}E(0) = \mathcal{D}E_0,\\
\mathbf{s}^0 &:= \mathcal{D}I(0) = \mathcal{D}I_0,\\
\mathbf{s}^0 &:= \mathcal{D}V(0) = \mathcal{D}V_0,\\
\mathbf{s}^0 &:= \mathcal{D}R(0) = \mathcal{D}R_0.
\end{aligned}\right\} \tag{32}$$

First-order problem

$$\left.\begin{aligned}
\mathbf{s}^1 &:= \mathcal{D}S_1 = \mu - qS(0)I(0) - (\omega + a)S(0) + \nu R(0),\\
\mathbf{s}^1 &:= \mathcal{D}E_1 = qS(0)I(0) - (c + \omega + a)E(0),\\
\mathbf{s}^1 &:= \mathcal{D}I_1 = cE(0) - (a + \omega + x + z)I(0),\\
\mathbf{s}^1 &:= \mathcal{D}V_1 = aI(0) - (\omega + y)V(0) + aE(0) + aS(0),\\
\mathbf{s}^1 &:= \mathcal{D}R_1 = xI(0) + yV(0) - (\omega + \nu)R(0).
\end{aligned}\right\} \tag{33}$$

Second-order problem

$$\left.\begin{aligned}
\mathbf{s}^2 &:= \mathcal{D}S_2 = -qS_1(t)I_1(t) - (\omega + a)S_1(t) + \nu R_1(t),\\
\mathbf{s}^2 &:= \mathcal{D}E_2 = qS_1(t)I_1(t) - (c + \omega + a)E_1(t),\\
\mathbf{s}^2 &:= \mathcal{D}I_2 = cE_1(t) - (a + \omega + x + z)I_1(t),\\
\mathbf{s}^2 &:= \mathcal{D}V_2 = aI_1(t) - (\omega + y)V_1(t) + aE_1(t) + aS_1(t),\\
\mathbf{s}^2 &:= \mathcal{D}R_2 = xI_1(t) + yV_1(t) - (\omega + \nu)R_1(t).
\end{aligned}\right\} \tag{34}$$

Third-order problem

$$\left.\begin{aligned}
\mathbf{s}^3 &:= \mathcal{D}S_3 = -qS_2(t)I_2(t) - (\omega + a)S_2(t) + \nu R_2(t),\\
\mathbf{s}^3 &:= \mathcal{D}E_3 = qS_2(t)I_2(t) - (c + \omega + a)E_2(t),\\
\mathbf{s}^3 &:= \mathcal{D}I_3 = cE_2(t) - (a + \omega + x + z)I_2(t),\\
\mathbf{s}^3 &:= \mathcal{D}V_3 = aI_2(t) - (\omega + y)V_2(t) + aE_2(t) + aS_2(t),\\
\mathbf{s}^3 &:= \mathcal{D}R_3 = xI_2(t) + yV_2(t) - (\omega + \nu)R_2(t).\\
&\vdots
\end{aligned}\right\} \tag{35}$$

nth-order problem

$$\left.\begin{aligned}
\mathbf{s}^{(n+1)} &:= \mathcal{D}S_{(n+1)} = -qS_{(n)}(t)I_{(n)}(t) - (\omega + a)S_{(n)}(t) + \nu R_{(n)}(t),\\
\mathbf{s}^{(n+1)} &:= \mathcal{D}E_{(n+1)} = qS_{(n)}(t)I_{(n)}(t) - (c + \omega + a)E_{(n)}(t),\\
\mathbf{s}^{(n+1)} &:= \mathcal{D}I_{(n+1)} = cE_{(n)}(t) - (a + \omega + x + z)I_{(n)}(t),\\
\mathbf{s}^{(n+1)} &:= \mathcal{D}V_{(n+1)} = aI_{(n)}(t) - (\omega + y)V_{(n)}(t) + aE_{(n)}(t) + aS_{(n)}(t),\\
\mathbf{s}^{(n+1)} &:= \mathcal{D}R_{(n+1)} = xI_{(n)}(t) + yV_{(n)}(t) - (\omega + \nu)R_{(n)}(t).
\end{aligned}\right\} \tag{36}$$

Next, system of equations (33) becomes:

$$\left.\begin{aligned}
S_1(t) &= (\mu - qS_0I_0 - (\omega + a)S_0 + \nu R_0)t,\\
E_1(t) &= (qS_0I_0 - (c + \omega + a)E_0)t,\\
I_1(t) &= (cE_0 - (a + \omega + x + z)I_0)t,\\
V_1(t) &= (aI_0 - (\omega + y)V_0 + aE_0 + aS_0)t,\\
R_1(t) &= (xI_0 + yV_0 - (\omega + \nu)R_0)t.
\end{aligned}\right\} \tag{37}$$

Next, system of equations (34) becomes:

$$\left.\begin{aligned} S_2(t) &= (-q(E_0c - I_0(a+\omega+x+z))(\mu + R_0\nu - S_0(a+\omega) - I_0S_0q))t^3 \\ &\quad + (\nu(I_0x + V_0y - R_0(\nu+\omega)) - (a+\omega)(\mu + R_0\nu - S_0(a+\omega) - I_0S_0q))t^2, \\ E_2(t) &= (q(E_0c - I_0(a+\omega+x+z))(\mu + R_0\nu - S_0(a+\omega) - I_0S_0q))t^3 \\ &\quad + ((E_0(a+c+\omega) - I_0S_0q)(a+c+\omega))t^2, \\ I_2(t) &= (-(E_0c - I_0(a+\omega+x+z))(a+\omega+x+z) - c(E_0(a+c+\omega) - I_0S_0q))t^2, \\ V_2(t) &= (a(E_0c - I_0(a+\omega+x+z)) - a(E_0(a+c+\omega) - I_0S_0q) - (\omega+y)(E_0a \\ &\quad + I_0a + S_0a - V_0(\omega+y)) + a(\mu + R_0\nu - S_0(a+\omega) - I_0S_0q))t^2, \\ R_2(t) &= (x(E_0c - I_0(a+\omega+x+z)) - (\nu+\omega)(I_0x + V_0y - R_0(\nu+\omega)) \\ &\quad + y(E_0a + I_0a + S_0a - V_0(\omega+y)))t^2. \end{aligned}\right\} \tag{38}$$

Next, system of equations (35) becomes:

$$\left.\begin{aligned} S_3(t) &= (-q^2\alpha_5\alpha_2\alpha_3)t^6 + (q\alpha_1\alpha_2)t^5 + (q(a+\omega)\alpha_5\alpha_3)t^4 + (\nu(x\alpha_5 - (\nu+\omega)\alpha_4 \\ &\quad + y(E_0a + I_0a + S_0a - V_0(\omega+y))) - (a+\omega)\alpha_1)t^3, \end{aligned}\right\} \tag{39}$$

where,

$$\left.\begin{aligned} \alpha_1 &= \nu\alpha_4 - (a+\omega)\alpha_3, \\ \alpha_2 &= \alpha_5(a+\omega+x+z) + c(E_0(a+c+\omega) - I_0S_0q), \\ \alpha_3 &= \mu + R_0\nu - S_0(a+\omega) - I_0S_0q, \\ \alpha_4 &= I_0x + V_0y - R_0(\nu+\omega), \\ \alpha_5 &= E_0c - I_0(a+\omega+x+z). \end{aligned}\right\} \tag{40}$$

$$\begin{aligned} E_3(t) &= (q^2\kappa_3\kappa_2\kappa_1)t^6 + (-q(\nu(I_0x + V_0y - R_0(\nu+\omega)) - (a+\omega)\kappa_1)\kappa_2)t^5 \\ &\quad + (-q\kappa_3(a+c+\omega)\kappa_1)t^4 + (-\kappa_4(a+c+\omega)^2)t^3, \end{aligned} \tag{41}$$

where,

$$\left.\begin{aligned} \kappa_1 &= \mu + R_0\nu - S_0(a+\omega) - I_0S_0q, \\ \kappa_2 &= \kappa_3(a+\omega+x+z) + c\kappa_4, \\ \kappa_3 &= E_0c - I_0(a+\omega+x+z), \\ \kappa_4 &= E_0(a+c+\omega) - I_0S_0q. \end{aligned}\right\} \tag{42}$$

$$I_3(t) = (cq\tau_2(\mu + R_0\nu - S_0(a+\omega) - I_0S_0q))t^4 + ((\tau_2(a+\omega+x+z) + c\tau_1)(a+\omega+x+z) + c\tau_1(a+c+\omega))t^3, \tag{43}$$

where,

$$\left.\begin{aligned} \tau_1 &= E_0(a+c+\omega) - I_0S_0q, \\ \tau_2 &= E_0c - I_0(a+\omega+x+z). \end{aligned}\right\} \tag{44}$$

$$\begin{aligned} V_3(t) &= (a(\nu(I_0x + V_0y - R_0(\nu+\omega)) - (a+\omega)\phi_2) - a(\phi_3(a+\omega+x+z) + c\phi_1) \\ &\quad + (\omega+y)((\omega+y)(E_0a + I_0a + S_0a - V_0(\omega+y)) + a\phi_1 - a\phi_3 - a\phi_2) + a\phi_1(a+c+\omega))t^3, \end{aligned} \tag{45}$$

where,

$$\left.\begin{aligned} \phi_1 &= E_0(a+c+\omega) - I_0S_0q, \\ \phi_2 &= \mu + R_0\nu - S_0(a+\omega) - I_0S_0q, \\ \phi_3 &= E_0c - I_0(a+\omega+x+z). \end{aligned}\right\} \tag{46}$$

$$\begin{aligned} R_3(t) &= (-y((\omega+y)\sigma_2 + a\sigma_3 - a\sigma_1 - a(\mu + R_0\nu - S_0(a+\omega) - I_0S_0q)) - (\nu+\omega)(x\sigma_1 \\ &\quad - (\nu+\omega)(I_0x + V_0y - R_0(\nu+\omega)) + y\sigma_2) - x(\sigma_1(a+\omega+x+z) + c\sigma_3))t^3, \end{aligned} \tag{47}$$

where,

$$\left.\begin{aligned}\sigma_1 &= E_0c - I_0(a+\omega+x+z),\\ \sigma_2 &= E_0a + I_0a + S_0a - V_0(\omega+y),\\ \sigma_3 &= E_0(a+c+\omega) - I_0S_0q.\end{aligned}\right\} \tag{48}$$

The resultant solution to model (2) is obtained as:

$$\left.\begin{aligned}S(t) &= (-q^2\alpha_5\alpha_2\alpha_3)t^6 + (q\alpha_1\alpha_2)t^5 + (q(a+\omega)\alpha_5\alpha_3)t^4 + (\nu(x\alpha_5 - (\nu+\omega)\alpha_4\\ &\quad + y(E_0a + I_0a + S_0a - V_0(\omega+y))) - (a+\omega)\alpha_1 - q\alpha_5\alpha_3)t^3 + \alpha_1t^2 + \alpha_3t + S_0,\\ E(t) &= (q^2\kappa_3\kappa_2\kappa_1)t^6 + (-q(\nu(I_0x + V_0y - R_0(\nu+\omega)) - (a+\omega)\kappa_1)\kappa_2)t^5 + (-q\kappa_3(a+c+\omega)\kappa_1)t^4\\ &\quad + (q\kappa_3\kappa_1 - \kappa_4(a+c+\omega)^2)t^3 + (\kappa_4(a+c+\omega))t^2 + (I_0S_0q - \kappa_5)t + E_0,\\ I(t) &= (cq\tau_1(\mu + R_0\nu - S_0(a+\omega) - I_0S_0q))t^4 + ((\tau_1(a+\omega+x+z) + c\tau_2)(a+\omega+x+z)\\ &\quad + c\tau_2(a+c+\omega))t^3 + (-\tau_1(a+\omega+x+z) - c\tau_2)t^2 + \tau_1t + I_0,\\ V(t) &= (a(\nu(I_0x + V_0y - R_0(\nu+\omega)) - (a+\omega)\phi_3) - a(\phi_4(a+\omega+x+z) + c\phi_1)\\ &\quad + (\omega+y)((\omega+y)\phi_2 + a\phi_1 - a\phi_4 - a\phi_3) + a\phi_1(a+c+\omega))t^3 + (a\phi_4 - a\phi_1\\ &\quad - (\omega+y)\phi_2 + a\phi_3)t^2 + \phi_2t + V_0,\\ R(t) &= (-y((\omega+y)\sigma_4 + a\sigma_1 - a\sigma_3 - a(\mu + R_0\nu - S_0(a+\omega) - I_0S_0q)) - (\nu+\omega)\sigma_2\\ &\quad - x(\sigma_3(a+\omega+x+z) + c\sigma_1))t^3 + \sigma_2t^2 + \sigma_5t + R_0.\end{aligned}\right\} \tag{49}$$

Furthermore, we present the following plots based on solution (49) in the graphical justification such that:

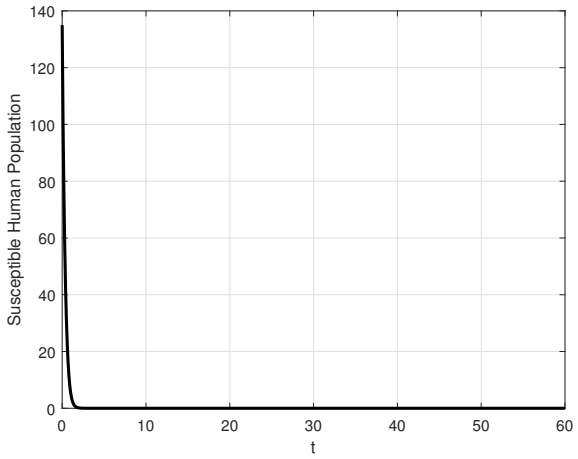

Figure 9. The plot shows the numerical simulation of susceptible human population, $S(t)$.

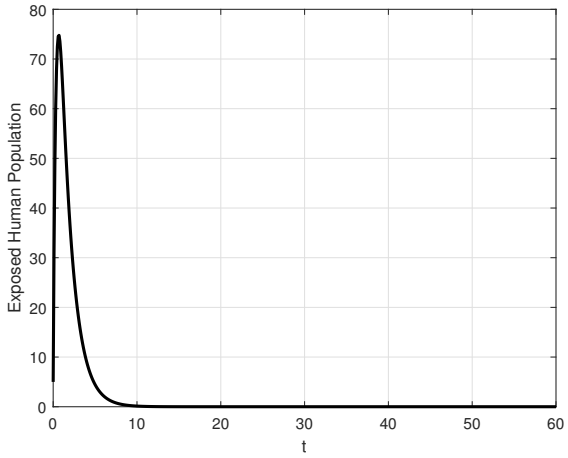

Figure 10. The plot shows the numerical simulation of exposed human population, $E(t)$.

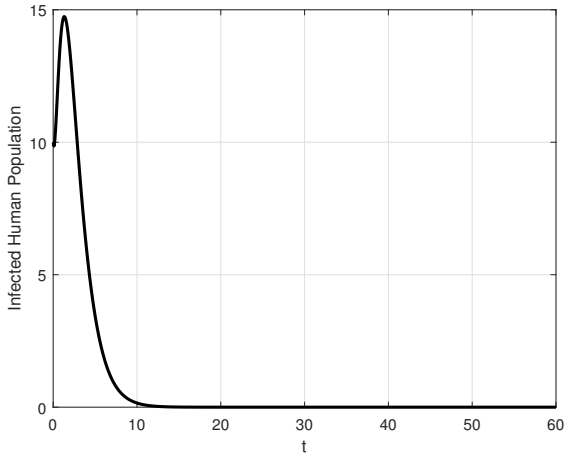

Figure 11. The plot shows the numerical simulation of infected human population, $I(t)$.

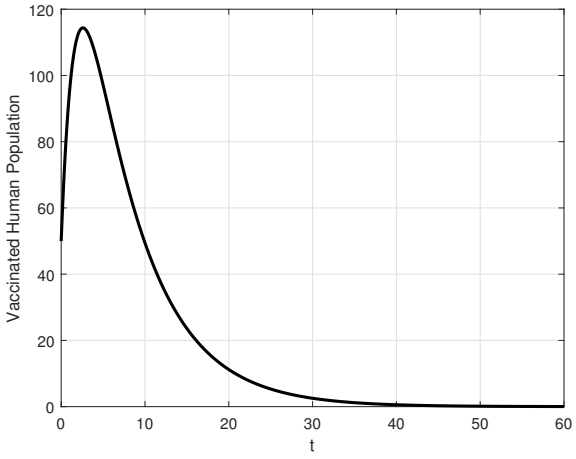

Figure 12. The plot shows the numerical simulation of vaccinated human population, $V(t)$.

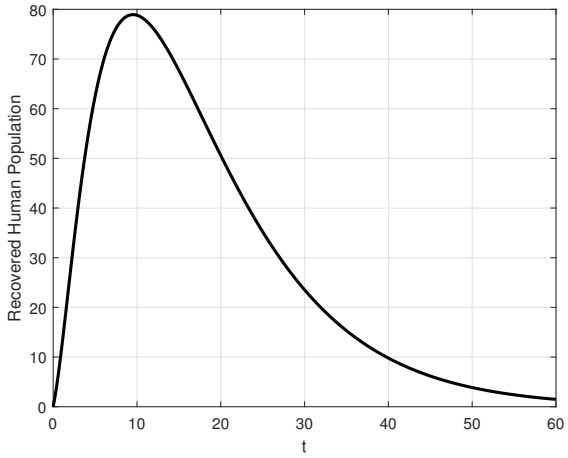

Figure 13. The plot shows the numerical simulation of recovered human population, $R(t)$.

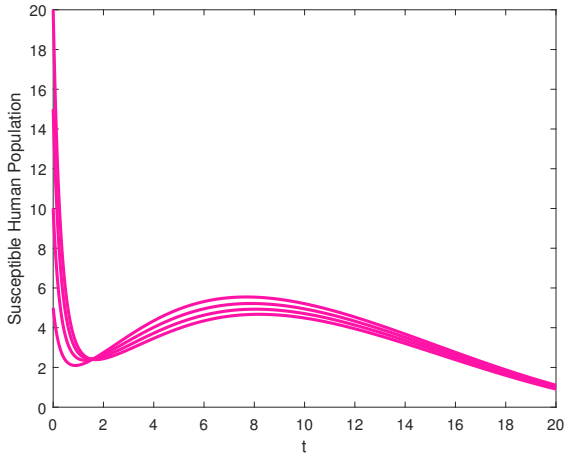

Figure 14. The plot shows the numerical simulation of susceptible human population, $R(t)$ with asymptotic stability graphically.

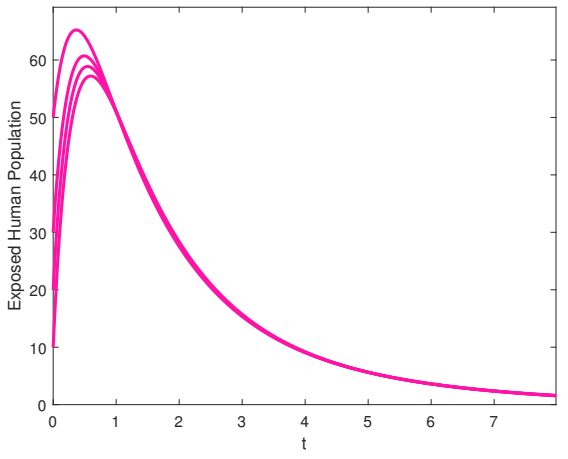

Figure 15. The plot shows the numerical simulation of exposed human population, $E(t)$ with asymptotic stability graphically.

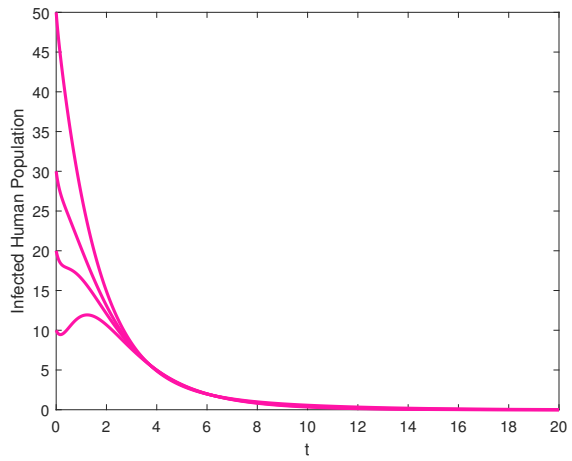

Figure 16. The plot shows the numerical simulation of infected human population, $I(t)$ with asymptotic stability graphically.

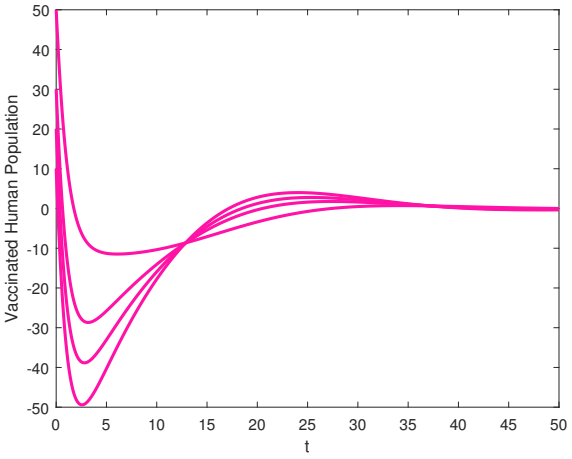

Figure 17. The plot shows the numerical simulation of vaccinated human population, $V(t)$ with asymptotic stability graphically.

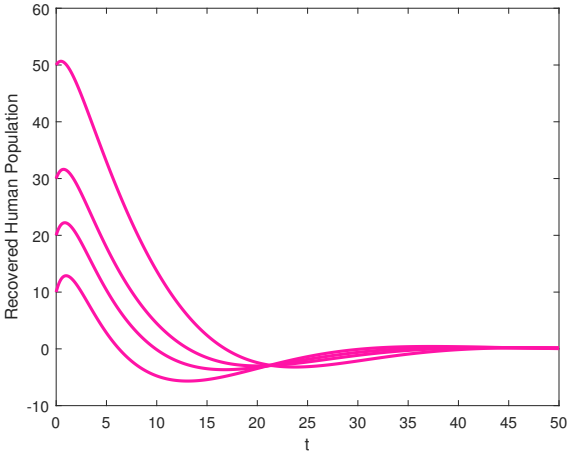

Figure 18. The plot shows the numerical simulation of recovered human population, $R(t)$ with asymptotic stability graphically.

Table 1. Table of description and initial condition of compartment of population

Symbol of Compartment	Description of Compartment	Initial Condition
$S(t)$	Susceptible Human Population	$N-(E+I+V+R)$
$E(t)$	Exposed Human Population	10
$I(t)$	Infected Human Population	20
$V(t)$	Vaccinated Human Population	30
$R(t)$	Recovered Human Population	0
N	Total Population	200

Table 2. Table of description and values of parameters

Symbol	Description of Parameter	Unit	Value
ω	Natural Death Rate	day^{-1}	$\frac{1}{67.7\times 365}$
μ	Recruitment Rate	day^{-1}	$\omega \times N$
q	Transmission rate	day^{-1}	0.2784
a	Vaccination Rate	day^{-1}	0.5
ν	Lose of Immunity in Recovered Population	day^{-1}	0.1
c	Rate of Infection of Exposed Population	day^{-1}	0.23
x	Recovery Rate of Infected Population	day^{-1}	0.05
y	Recovery Rate of Vaccinated Population	day^{-1}	0.15
z	Death Rate of Infected Population due to COVID−19 Infection	day^{-1}	0.32

6 Results and discussion

We discuss the outcomes of the stability analysis of COVID−19 at both disease-free and endemic equilibrium points, the spread of the infection is asymptotically stable locally and globally under certain conditions such that $F < \alpha$. For global stability analysis the Lyapunov function is used at disease free and endemic equilibrium points. The Lyapunov function is negative is $F < \alpha$ so it means that the spread of infection will be stable and will not be spread in the population so it cannot lead to a pandemic. After the recent invention of the vaccination, we implemented the vaccinated individuals compartment $V(t)$ also the Figure (12) which is the graphical behaviour. We discuss the outcomes of the Homotopy Perturbation Method by applying it to the COVID−19 model, (2). In Figure (9), the dynamics of susceptible human population ion has been shown in which the population decreases with time due to the large transmission b and vaccination a rates. In Figure (10), the plot shows the dynamics of the Exposed Human population in which the population increased in the first week while then decreased asymptotically. In Figure (11), in the first two weeks, the prevalence increased due to the higher rate of transmission and infectivity, and then the disease disappeared from the population thus the prevalence decreasing to zero. In Figures (12) and (13), the dynamics of the Vaccinated and Recovered populations have been shown. While the Figures (14), (15), (16), (17), and (18) give the asymptotically stable behaviour of Susceptible, Exposed, Infected, Vaccinated, and Recovered Populations, respectively by varying the initial conditions for each class of the model (2).

7 Conclusion

In this paper, we studied the stability of the COVID−19 model which is locally and globally asymptotically stable around the disease-free and endemic equilibrium points by having negative eigenvalues at both disease-free and endemic equilibrium points satisfying Routh−Hurwitz criterion. Global stability is investigated with the help of Lyapunov function. The disease is locally asymptotically stable at disease−free equilibrium point if $R_0 < 1$ while unstable if $R_0 > 1$ likewise, at endemic−equilibrium point if $R_0 > 1$ while unstable if $R_0 < 1$. Looking for the behaviour of the vaccination in population, it has a positive impact on population and ability to protect the population from re−infection and future pandemics. Individual vaccination, rapid diagnosis, and possibly early treatment are the most effective ways to prevent coronavirus infection in the community. As is generally known, the COVID-19 infection has caused significant damage to human society, with many developing countries experiencing significant financial losses. As a result, adequate individual vaccines and infection control should be a priority for less developed countries in order to sustain their populations and economies. On analyzing the semi-analytic solution of the COVID−19 models using the homotopy perturbation method, we have obtained that the homotopy perturbation method is efficient, powerful, and more accurate and is capable of obtaining a semi-analytic solution that is both linear and non−linear as well. This method can be applied to ordinary differential equations in integer-order and fractional orders too, partial differential equations, and boundary value problems. The said method can be applied to the system of many differential equations and higher-order problems. In all scenarios, the solution can be obtained semi-analytically and more accurately.

Declarations

Consent for publication

Not applicable.

Conflicts of interest

The authors declare that they have no known competing financial interests or personal relationships that could have appeared to influence the work reported in this paper.

Author's contributions

M.S.: Writing-Original draft preparation, Validation, Conceptualization, Methodology, Software. J.L.: Supervision, Validation, Conceptualization, Methodology, Investigation, Software. M.A.: Writing-Original draft preparation, Methodology. M.F.: Visualization, Methodology, Writing–Reviewing and Editing. All authors discussed the results and contributed to the final manuscript.

Acknowledgements

Not applicable.

References

[1] https://www.worldometers.info/coronavirus/, Coronavirus cases. Access Date: 20.06.2022
[2] Sinan, M., Ali, A., Shah, K., Assiri, T.A., & Nofal, T.A. Stability analysis and optimal control of COVID-19 pandemic SEIQR fractional mathematical model with harmonic mean type incidence rate and treatment. *Results in Physics*, 22, 103873, (2021). [CrossRef]
[3] Ali, A., Khan, M.Y., Sinan, M., Allehiany, F.M., Mahmoud, E.E., Abdel-Aty, A.H., & Ali, G. Theoretical and numerical analysis of novel COVID-19 via fractional order mathematical model. *Results in physics*, 20, 103676, (2021). [CrossRef]
[4] Asamoah, J.K.K., Owusu, M.A., Jin, Z., Oduro, F.T., Abidemi, A., & Gyasi, E.O. Global stability and cost-effectiveness analysis of COVID-19 considering the impact of the environment: using data from Ghana. *Chaos, Solitons & Fractals*, 140, 110103, (2020). [CrossRef]
[5] Péni, T., Csutak, B., Szederkényi, G., & Röst, G. Nonlinear model predictive control with logic constraints for COVID-19 management. *Nonlinear Dynamics*, 102(4), 1965-1986, (2020). [CrossRef]
[6] Matouk, A.E. Complex dynamics in susceptible-infected models for COVID-19 with multi-drug resistance. *Chaos, Solitons & Fractals*, 140, 110257, (2020). [CrossRef]
[7] Sun, D., Duan, L., Xiong, J., & Wang, D. Modeling and forecasting the spread tendency of the COVID-19 in China. *Advances in Difference Equations*, 2020(1), 1-16, (2020). [CrossRef]
[8] Ahmed, I., Baba, I.A., Yusuf, A., Kumam, P., & Kumam, W. Analysis of Caputo fractional-order model for COVID-19 with lockdown. *Advances in difference equations*, 2020(1), 1-14, (2020). [CrossRef]
[9] Alqahtani, R.T. Mathematical model of SIR epidemic system (COVID-19) with fractional derivative: stability and numerical analysis. *Advances in Difference Equations*, 2021(1), 1-16, (2021). [CrossRef]
[10] Naik, P.A., Zu, J., & Owolabi, K.M. Global dynamics of a fractional order model for the transmission of HIV epidemic with optimal control. *Chaos, Solitons & Fractals*, 138, 109826, (2020). [CrossRef]
[11] Zhu, L., Zhou, X., Li, Y., & Zhu, Y. Stability and bifurcation analysis on a delayed epidemic model with information-dependent vaccination. *Physica scripta*, 94(12), 125202, (2019). [CrossRef]
[12] Allegretti, S., Bulai, I.M., Marino, R., Menandro, M.A., & Parisi, K. Vaccination effect conjoint to fraction of avoided contacts for a Sars-Cov-2 mathematical model. *Mathematical Modelling and Numerical Simulation with Applications*, 1(2), 56-66, (2021). [CrossRef]
[13] Shah, K., Abdeljawad, T., Mahariq, I., & Jarad, F. Qualitative analysis of a mathematical model in the time of COVID-19. *BioMed Research International*, 2020, (2020). [CrossRef]
[14] Pais, R.J., & Taveira, N. Predicting the evolution and control of the COVID-19 pandemic in Portugal. *F1000Research*, 9, (2020). [CrossRef]
[15] Martcheva, M. *An introduction to mathematical epidemiology* (Vol. 61, pp. 9-31). New York: Springer, (2015).
[16] Samji, H., Wu, J., Ladak, A., Vossen, C., Stewart, E., Dove, N., ... & Snell, G. Mental health impacts of the COVID-19 pandemic on children and youth–a systematic review. *Child and adolescent mental health*, 27(2), 173-189, (2022). [CrossRef]
[17] Li, X.P., Gul, N., Khan, M.A., Bilal, R., Ali, A., Alshahrani, M.Y., ... & Islam, S. A new Hepatitis B model in light of asymptomatic carriers and vaccination study through Atangana–Baleanu derivative. *Results in Physics*, 29, 104603, (2021). [CrossRef]
[18] Din, A., & Li, Y. Stationary distribution extinction and optimal control for the stochastic hepatitis B epidemic model with partial immunity. *Physica Scripta*, 96(7), 074005, (2021). [CrossRef]
[19] Din, A., & Li, Y. Lévy noise impact on a stochastic hepatitis B epidemic model under real statistical data and its fractal–fractional Atangana–Baleanu order model. *Physica Scripta*, 96(12), 124008, (2021). [CrossRef]
[20] Din, A., Li, Y., Khan, F.M., Khan, Z.U., & Liu, P. On Analysis of fractional order mathematical model of Hepatitis B using Atangana–Baleanu Caputo (ABC) derivative. *Fractals*, 30(01), 2240017, (2022). [CrossRef]
[21] Din, A., Li, Y., Yusuf, A., & Ali, A.I. Caputo type fractional operator applied to Hepatitis B system. *Fractals*, 30(01), 2240023, (2022). [CrossRef]
[22] Din, A., & Abidin, M.Z. Analysis of fractional-order vaccinated Hepatitis-B epidemic model with Mittag-Leffler kernels. *Mathematical Modelling and Numerical Simulation with Applications*, 2(2), 59-72, (2022). [CrossRef]
[23] Ali, A., Alshammari, F.S., Islam, S., Khan, M.A., & Ullah, S. Modeling and analysis of the dynamics of novel coronavirus (COVID-19) with Caputo fractional derivative. *Results in Physics*, 20, 103669, (2021). [CrossRef]
[24] Daşbaşı, B. Stability analysis of an incommensurate fractional-order SIR model. *Mathematical Modelling and Numerical Simulation with Applications*, 1(1), 44-55, (2021). [CrossRef]
[25] Ali, A., Islam, S., Khan, M.R., Rasheed, S., Allehiany, F.M., Baili, J., ... & Ahmad, H. Dynamics of a fractional order Zika virus model with mutant. *Alexandria Engineering Journal*, 61(6), 4821-4836, (2022). [CrossRef]
[26] Ali, A., Iqbal, Q., Asamoah, J.K.K., & Islam, S. Mathematical modeling for the transmission potential of Zika virus with optimal control strategies. *The European Physical Journal Plus*, 137(1), 1-30, (2022). [CrossRef]
[27] Zhang, X.H., Ali, A., Khan, M.A., Alshahrani, M.Y., Muhammad, T., & Islam, S. Mathematical analysis of the TB model with treatment via Caputo-type fractional derivative. *Discrete Dynamics in Nature and Society*, 2021, (2021). [CrossRef]
[28] Faniran, T., Ali, A., Adewole, M.O., Adebo, B., & Akanni, O.O. Asymptotic behavior of tuberculosis between smokers and non-smokers. *Partial Differential Equations in Applied Mathematics*, 5, 100244, (2022). [CrossRef]
[29] Din, A., & Li, Y. The extinction and persistence of a stochastic model of drinking alcohol. *Results in Physics*, 28, 104649, (2021). [CrossRef]

[30] Naik, P.A., Eskandari, Z., Yavuz, M., & Zu, J. Complex dynamics of a discrete-time Bazykin–Berezovskaya prey-predator model with a strong Allee effect. *Journal of Computational and Applied Mathematics*, 413, 114401, (2022). [CrossRef]
[31] Abdy, M., Side, S., Annas, S., Nur, W., & Sanusi, W. An SIR epidemic model for COVID-19 spread with fuzzy parameter: the case of Indonesia. *Advances in difference equations*, 2021(1), 1-17, (2021). [CrossRef]
[32] Yavuz, M., Coşar, F.Ö., Günay, F., & Özdemir, F.N. A new mathematical modeling of the COVID-19 pandemic including the vaccination campaign. *Open Journal of Modelling and Simulation*, 9(3), 299-321, (2021). [CrossRef]
[33] Özköse, F., Yavuz, M., Şenel, M.T., & Habbireeh, R. Fractional order modelling of omicron SARS-CoV-2 variant containing heart attack effect using real data from the United Kingdom. *Chaos, Solitons & Fractals*, 157, 111954, (2022). [CrossRef]
[34] Shen, Z.H., Chu, Y.M., Khan, M.A., Muhammad, S., Al-Hartomy, O.A., & Higazy, M. Mathematical modeling and optimal control of the COVID-19 dynamics. *Results in Physics*, 31, 105028, (2021). [CrossRef]
[35] Ahmad, S., Ullah, A., Al-Mdallal, Q.M., Khan, H., Shah, K., & Khan, A. Fractional order mathematical modeling of COVID-19 transmission. *Chaos, Solitons & Fractals*, 139, 110256, (2020). [CrossRef]
[36] Abdo, M.S., Shah, K., Wahash, H.A., & Panchal, S.K. On a comprehensive model of the novel coronavirus (COVID-19) under Mittag-Leffler derivative. *Chaos, Solitons & Fractals*, 135, 109867, (2020). [CrossRef]
[37] Robinson, E., Sutin, A.R., Daly, M., & Jones, A. A systematic review and meta-analysis of longitudinal cohort studies comparing mental health before versus during the COVID-19 pandemic in 2020. *Journal of affective disorders*, 296, 567-576, (2022). [CrossRef]
[38] Oud, M.A.A., Ali, A., Alrabaiah, H., Ullah, S., Khan, M.A., & Islam, S. A fractional order mathematical model for COVID-19 dynamics with quarantine, isolation, and environmental viral load. *Advances in Difference Equations*, 2021(1), 1-19, (2021). [CrossRef]
[39] Mathieu, E., et al. A global database of COVID-19 vaccinations. *Nature Human Behaviour,* 5(7), 947-953, (2021). [CrossRef]
[40] https://www.who.int/ Access Date: 20.06.2022
[41] He, J.H. Homotopy perturbation technique. *Computer methods in applied mechanics and engineering*, 178(3-4), 257-262, (1999). [CrossRef]
[42] He, J.H. Comparison of homotopy perturbation method and homotopy analysis method. *Applied Mathematics and Computation*, 156(2), 527-539, (2004). [CrossRef]
[43] Sinan, M., Shah, K., Khan, Z.A., Al-Mdallal, Q., & Rihan, F. On Semianalytical Study of Fractional-Order Kawahara Partial Differential Equation with the Homotopy Perturbation Method. *Journal of Mathematics*, 2021, (2021). [CrossRef]
[44] Mohyud-Din, S.T., & Noor, M.A. Homotopy perturbation method for solving partial differential equations. *Zeitschrift für Naturforschung A*, 64(3-4), 157-170, (2009). [CrossRef]
[45] Sinan, M. Analytic approximate solution of rabies transmission dynamics using homotopy perturbation method. *Matrix Science Mathematics (MSMK)*, 4(1), 01-05, (2020). [CrossRef]
[46] Zedan, H.A., & El Adrous, E. The application of the homotopy perturbation method and the homotopy analysis method to the generalized Zakharov equations. *In Abstract and Applied Analysis*, 2012, (2012). [CrossRef]
[47] Demir, A., Erman, S., Özgür, B., & Korkmaz, E. Analysis of the new homotopy perturbation method for linear and nonlinear problems. *Boundary Value Problems*, 2013(1), 1-11, (2013). [CrossRef]
[48] Zhang, Z., ur Rahman, G., Gómez-Aguilar, J.F., & Torres-Jiménez, J. Dynamical aspects of a delayed epidemic model with subdivision of susceptible population and control strategies. *Chaos, Solitons & Fractals*, 160, 112194, (2022). [CrossRef]
[49] Wang, Z., Nie, X., & Liao, M. Stability Analysis of a Fractional-Order SEIR-KS Computer Virus-Spreading Model with Two Delays. *Journal of Mathematics*, 2021, (2021). [CrossRef]

Mathematical Modelling and Numerical Simulation with Applications (MMNSA) (https://www.mmnsa.org)